Check for updates

Received: 27 March 2021 | Accepted: 28 March 2021

DOI: 10.1002/mmce.22859

RESEARCH ARTICLE

INTERNATIONAL JOURNAL OF RF AND MICROWAVE COMPUTER-AIDED ENGINEERING WILEY

Circularly-polarized cavity-backed slot antenna array with simplified feeding structure

Rui-Sen Chen[1] | **Lei Zhu**[2] | **Sai-Wai Wong**[3] | **Xu-Zhou Yu**[3] | **Jing-Yu Lin**[4] | **Yin Li**[3] | **Yejun He**[3]

[1]School of AI-Guangdong & Taiwan, Foshan University, Foshan, China

[2]Department of Electrical and Computer Engineering, Faculty of Science and Technology, University of Macau, Macau SAR, China

[3]College of Electronics and Information Engineering, Shenzhen University, Shenzhen, China

[4]School of Electrical and Data Engineering, University of Technology Sydney, Ultimo, New South Wales, Australia

Correspondence
Sai-Wai Wong, Nanshan District, Nanhai Avenue 3688, Shenzhen University, Shenzhen, China.
Email: wongsaiwai@ieee.org

Funding information
Shenzhen University Research Startup Project of New Staff, Grant/Award Number: 860-000002110311; Shenzhen Science and Technology Program, Grant/Award Numbers: JSGG20180507183215520, GJHZ20180418190529516, JCYJ20190728151457763, JCYJ20180305124543176; Natural Science Foundation of Guangdong Province, Grant/Award Number: 2018A030313481; National Natural Science Foundation of China, Grant/Award Numbers: 61801299, 62071306

Abstract

A class of circularly-polarized cavity-backed slot antenna arrays with simplified feeding structure are proposed. Power dividing network is an essential feeding structure for the design of conventional antenna arrays, which results in complicated antenna structure. A novel feeding technique based on the electric field of cavity modes is introduced to feed the array elements. The slots on the top wall are directly fed by the electric field without additional feeding structure. Crossed slots with different lengths are introduced to achieve the self-phased CP radiation as they produce different perturbation on the two degenerate cavity modes. Therefore, high efficiency and simple antenna structure of the CP slot antenna array are achieved. Then, two CP slot arrays with 3×3 and 8×8 elements are presented to show the designed feasibility. Finally, the 3×3 CP antenna array is fabricated and measured to validate the design concept, which can achieve 12.6 dBic gain, 94% total efficiency, 80% aperture efficiency, and -25 dB cross polarization.

KEYWORDS

cavity-backed slot antenna arrays, circularly-polarized, crossed slots, high efficiency, simplified feeding structure

1 | INTRODUCTION

Cavity-backed slot antenna (CBSA) is a good candidate for the high-efficiency and high-gain wireless communication systems. SIW CBSAs designed in References 1-3 have low profile and low cost, but has low efficiency produced by dielectric loss. The air-filled SIW[4,5] can reduce the dielectric loss, which can be used to design efficiency-enhanced slot antennas.[6,7] In general, due to the involvement of the substrate, air-filled SIW slot antennas still have relatively lower efficiency compared with the full-metal slot antennas.[8-10] Besides, full-metal slot antennas are highly demanded in high-power communication systems for their high power-handling capacity.

Circularly polarized antennas are widely used in satellite and radar communication systems to reduce polarization mismatch and multi-path interference. The degenerate modes is a widely-used method to design CP antennas,[11-20] including CP patch antennas,[11-14] CP SIW slot antennas,[15-19] and metal cavity slot antenna.[20] This

 © 2021 Wiley Periodicals LLC.

design method results in a narrow AR bandwidth, the AR bandwidth of the CP antennas in References 11-20 were around 1%, and some CP antennas had AR bandwidth less than 0.5%.[11,13,19] These narrowband CP antennas have their own application. For instance, the navigation systems, such as GPS/GLONASS/Galileo, only needs a narrow CP bandwidth (less than 0.5%, the GPS band is less than 0.2%).

To improve the antenna gain, CP antenna arrays composed of multiple radiating elements were designed in References 18,21-26. In Reference 18, a two-layer 1-to-16 power dividing network was used to feed the 4×4 radiating elements and a layer of metallic waveguide polarizer was used to achieve the CP radiation. In Reference 25, a complicated feeding network with multiple-state power dividers was used to feed the array elements. The utilizations of power dividers, polarizers or phase shifters resulted in a complicated structure and an enlarged size. Besides, the energy dissipating on the feeding network may reduce the radiation efficiency.

In this article, a novel simplified feeding structure is proposed to design CP antenna slot array. The radiation slots placed on the top wall can be directly excited by the electric field of the cavity modes. Two degenerate cavity modes perturbed by the cross-slots are introduced to achieve the CP radiation. By these means, all the CP radiation elements (cross-slots) can be directly fed without any power dividers and phase shifters, which can significantly reduce the antenna complexity and design complexity. Then, two CP antenna arrays with 3×3 and 8×8 elements are designed based on the proposed design concept. The 8×8 CP array can achieve 99.5% radiation efficiency. Finally, the 3×3 CP antenna array is fabricated and measured to validate the concept. In the measurement, the antenna can achieve 12.6 dBic gain, 94% total efficiency and 80% aperture efficiency.

2 | CIRCULARLY-POLARIZED CAVITY-BACKED CROSS-SLOT ANTENNA

The basic principle of the CP antenna with single feeding point is to produce two degenerate modes with 90° phase difference. We firstly consider the single-element CP slot antenna shown in Figure 1, of which the cutting XY-plane is in a square shape. The feeding slot, feeding cavity and probe are combined to form a coaxial-to-waveguide transition, which is used to excite cavity modes. The rotated cross-slot with different sizes is used to achieve the CP radiation property.

Based on the equivalent circuit of CP rectangular patch antenna,[27] the equivalent *LC*-circuit model of the

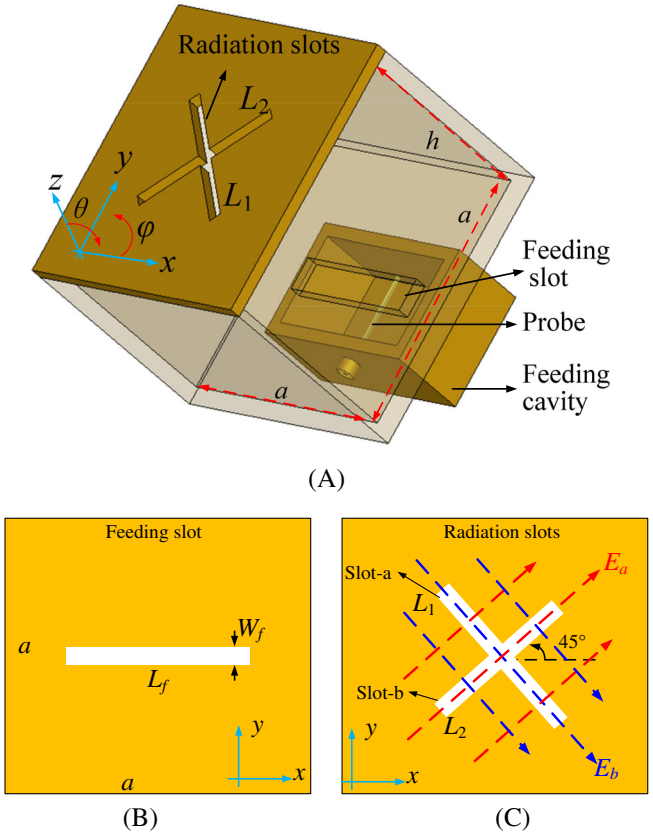

FIGURE 1 Proposed CP cavity-backed rotated cross-slot antenna: (A) Perspective view; (B) Top-view; (C) Side view. Initial dimensions (Unit: mm): $a = 60$, $h = 49$, $L_1 = 38$, $L_2 = 38$, $W = 2.5$, $D_1 = 36.5$, $t_1 = 2.5$, $t_2 = 3$, $D_p = 5.5$, $W_f = 8$, $L_f = 39$, $L_p = 21$, $P = 48$, $q = 25$, $s = 25$

antenna is given in Figure 2A, which includes two branches corresponding to the two degenerate modes f_a and f_b. These two modes have electric field distributions E_a and E_b, respectively, as shown in Figure 1C. The shunt inductance L_r and capacitance C_r represent the *LC*-resonator model of the cavity modes TE_{101} and TE_{011} without any perturbation. C_f represents the loading capacitance of the feeding slots. This equivalent circuit can help to understand the operation mechanism of the proposed CP antenna, that is, how to individually control the resonant frequencies of the two degenerate modes to obtain desired 90° phase difference. The original resonant frequencies of them are calculated using Equation (1). The C_a and C_b represent the perturbations of Slot-*a* and Slot-*b* on f_a and f_b, respectively. The resonant frequencies of them under the effect of the cross-slot are calculated as (2a) and (2b), respectively.

If the sizes of Slot-*a* and Slot-*b* are equal, that is, $L_1 = L_2$, we obtain that $C_a = C_b$ and $f_a = f_b$. Thus, these two modes have equal resonant frequency and excitation phase, as can be seen from Figure 2B, which indicates that the antenna is linearly polarized.

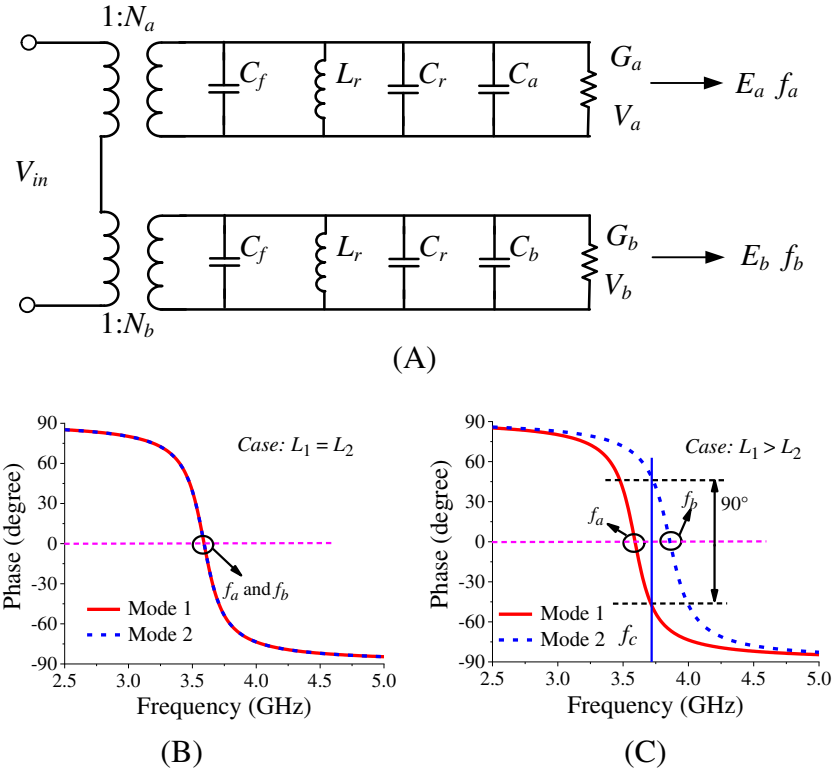

FIGURE 2 Realization of the CP property of the proposed cavity-backed rotated cross slots: (A) Equivalent circuit model after perturbation by the slots, (B) Phase performance under condition of $L_1 = L_2$; (C) Phase performance under condition of $L_1 > L_2$

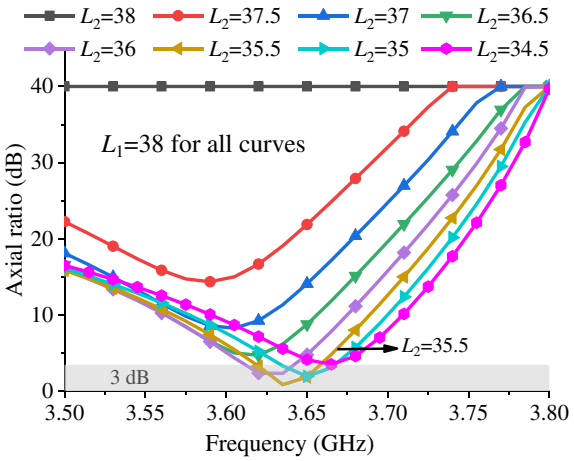

FIGURE 3 Simulated axial ratio against the slot length L_2

$$f_r = \frac{1}{2\pi\sqrt{L_r C_r}} = \frac{v}{2}\sqrt{\left(\frac{1}{a}\right)^2 + \left(\frac{1}{h}\right)^2} \tag{1}$$

$$f_a = \frac{1}{2\pi\sqrt{L_r\left(C_f + C_r + C_a\right)}} \tag{2a}$$

$$f_b = \frac{1}{2\pi\sqrt{L_r\left(C_f + C_r + C_b\right)}} \tag{2b}$$

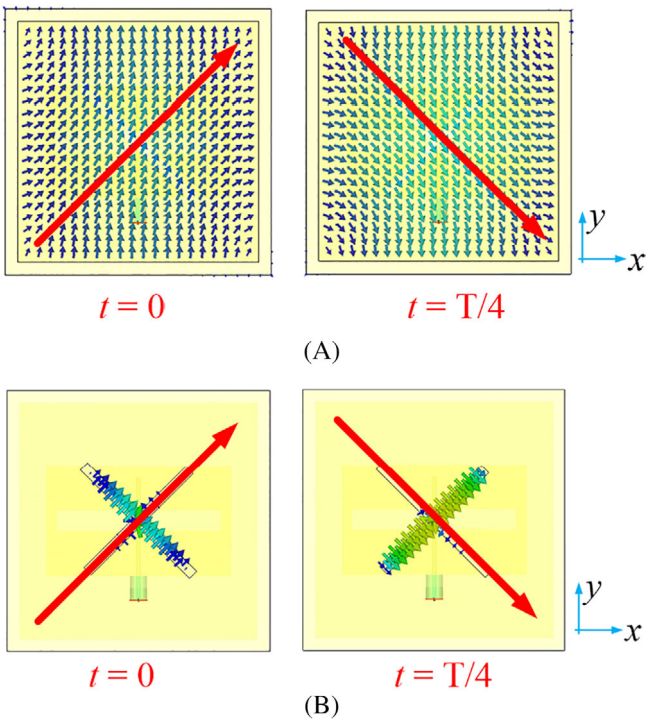

FIGURE 4 Electric field distribution at different time instances for $L_1 = 38$ mm and $L_2 = 35.5$ mm (at AR minima in Figure 2): (A) At the XY-plane with a depth of $h/2$; (B) At top wall

Next, the case of the different slots' sizes is investigated. The decreasing length of the Slot-b (L_2) means a decreasing C_b. and an increasing f_b is obtained according

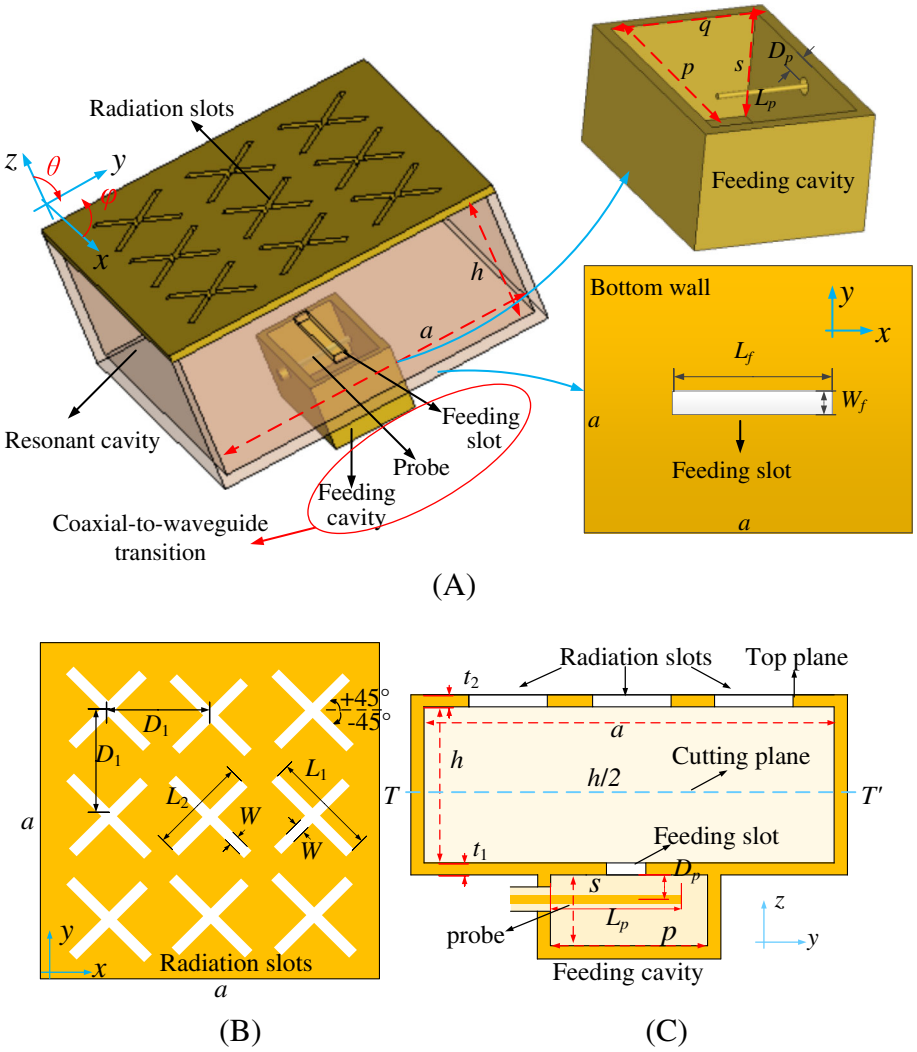

FIGURE 5 Proposed CP cavity-backed rotated cross-slot antenna array: (A) Perspective view; (B) Top-view; (C) Side view. Initial dimensions (Unit: mm): $a = 120$, $h = 49$, $L_1 = 38$, $L_2 = 38$, $W = 2.5$, $D_1 = 36.5$, $t_1 = 2.5$, $t_2 = 3$, $D_p = 5.5$, $W_f = 8$, $L_f = 39$, $L_p = 21$, $P = 48$, $q = 25$, $s = 25$

to the Equation (2b). Thus, f_b is higher than f_a. This frequency difference can produce a phase difference at the frequency between the two resonances. By properly modifying L_2, a 90° phase difference can be obtained at f_c, as shown in Figure 2C, which consequently generates the CP radiation. To prove the previous analysis, the simulated AR versus different L_2 is shown in Figure 3. It can be seen that the AR over the frequency is infinite (defined as AR = 40 dB) under the case of $L_1 = L_2 = 38$ mm, which means that the antenna is linearly polarized. A better AR is achieved when the L_2 is decreased from 38 to 35.5 mm, as the phase difference is increased to approximately 90°, and approximately-equal amplitude is remained. It can be also predicted that when L_2 is decreased to 0 mm, the antenna returns to linear polarization.

To directly understand the CP radiation, the electric field distributions at the XY-plane ($h/2$ depth) and on the top wall at AR minima are provided in Figure 4. These two modes are a pair of degenerate modes, as they have orthogonal electric fields at −45° and +45° orientation, respectively. Besides, they have a 90° phase difference at adjacent quarter periods to achieve the CP radiation.

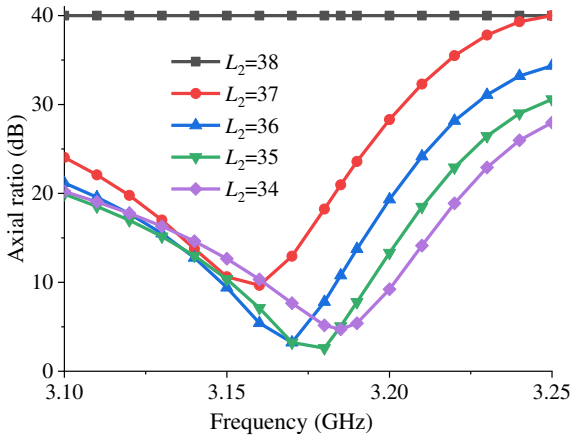

FIGURE 6 Simulated axial ratio against the slot length L_2

3 | CIRCULARLY-POLARIZED CAVITY-BACKED SLOT ANTENNA ARRAY

3.1 | Simplified feeding structure

After discussing the achievement of the CP radiation based on single feeding point and two crossed slots, we focus on the design of the circularly-polarized slot antenna array with simplified feeding structure. A 3×3 slot antenna array is firstly presented and designed, whose configuration is shown in Figure 5. The 3×3 rotated cross-slots are symmetrically placed on the top wall and form a 3×3 slot antenna array. All the radiation slots are fed by the electric field of the two degenerate modes without utilizing any power dividers and phase shifters. Among them, the 3×3 slot units with rotation angle of -45° are excited by the mode f_a with an electric field distribution E_a, while the 3×3 slot units with rotation angle of $+45^\circ$ are excited by the mode f_b with an electric field distribution E_b.

Similarly, the CP radiation is obtained under the condition of $L_1 \neq L_2$. To investigate the achievement of CP radiation of the 3×3 slot array, the simulated AR of the antenna versus different L_2 is shown in Figure 6. It can be seen that the AR over the frequency is infinite when $L_1 = L_2 = 38$ mm, and a low AR is obtained when the length of slots with $+45^\circ$ rotation, that is, L_2, is decreased from 38 to 35 mm.

The electric field distribution at the cutting plane ($h/2$ depth) and on the top wall at 3.17 GHz is provided in Figure 7. Figure 7A indicates that the two cavity modes are TE_{101} and TE_{011} with an inclined electric field distribution, and they have a 90° phase difference at adjacent quarter periods. Figure 7B shows the electric field distribution on the radiation slots. At time $t = 0$, all the slots with -45° rotation are directly and simultaneously excited and corresponded to the radiation, while at $t = T/4$, all the slots with $+45^\circ$ rotation are directly and simultaneously excited and corresponded to the radiation. This is an attractive advantage that no power divider is used to feed the array elements. This simplified feeding structure can reduce the structure complexity and design complexity.

3.2 | Parametric study

Then, the parametric study of the proposed CP slot antenna array is presented. The AR performance is mainly affected by the radiation slots. Figure 6 has shown the effect of the length of the radiation slots. Here, the effects of some other parameters are then studied. Figure 8 shows that the varying slot width W and spacing D_1 can slightly affect the AR. Thus, the AR performance of the CP slot array can be optimized by L_1, L_2, W, and D_1.

After analyzing AR performance, the impedance matching is then discussed. Figures 8 indicate that the varying dimensions have effect on AR as well as on the impedance matching. In fact, all the physical dimensions can affect the impedance matching, but not always affect the AR. Figure 9 shows that the increasing length of the feeding slot, that is, L_f, and the decreasing spacing between the probe and bottom wall, that is, D_p, can achieve a better impedance matching, while they have no effect on the AR performance. The reason is that they have same perturbation on the two degenerate modes. The dimensions of W_f, L_p, and t_1 shown in Figure 5 can be also used to optimize the impedance matching without affecting on the AR performance. Thus, the impedance matching of the proposed slot array can be individually optimized without affecting the AR performance, which gives the convenience in the design of the proposed CP antenna arrays.

3.3 | Antenna design and experimental results

Based on the above analysis, the design procedure of proposed CP slot array includes four main steps:

Step I: According to the operating frequency and Equation (1), the initial size of the resonant cavity is obtained.

Step II: Optimize the AR performance by adjusting the dimensions L_1, L_2, W, and D_1, as shown in Figures 6 and 9.

Step III: After obtaining the desired AR performance, the impedance matching is conducted by adjusting L_f, D_p, W_f, L_p, and t_1 without affecting the AR performance.

Step IV: The frequency shift during the optimization can be complemented by slightly modifying the cavity size.

Then, the proposed 3×3 CP antenna array is designed following the four steps. For proof-of-concept, the proposed 3×3 antenna array is fabricated and measured, and the photographs of the antenna and measurement setup are shown in Figure 10A,B, respectively. The comparison of simulated and measured results is shown in Figures 11 and 12. The center frequencies in the simulation and measurement are 3.18 and 3.172 GHz, respectively. The slight frequency offset is due to the fabrication roughness. The 10-dB impedance bandwidth and 3-dB AR bandwidth of the 3×3 array are 50 MHz/1.6% and 16 MHz/0.5%, respectively. The measured gain is 12.6 dBic, which is a little lower than the simulated one

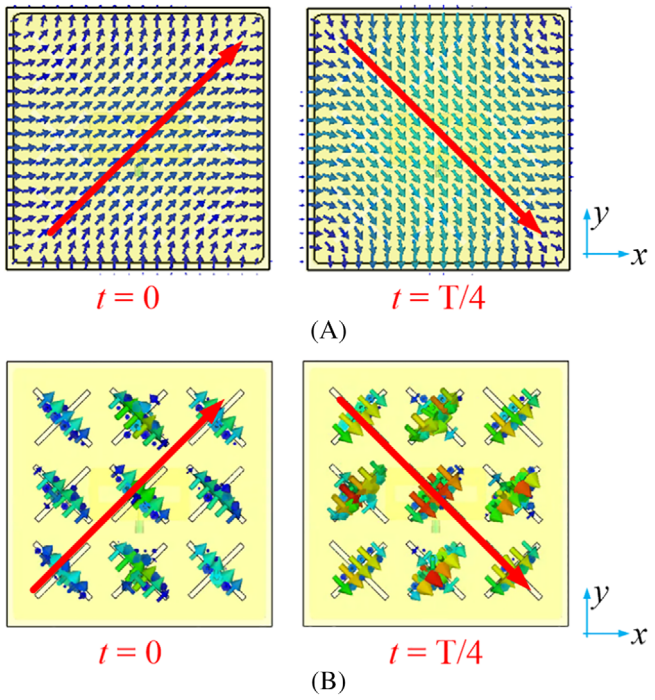

FIGURE 7 Electric field distribution at different time instances for $L_1 = 38$ mm and $L_2 = 35$ mm (at 3.17 GHz): (A) At the cutting plane $T - T'$ of a depth of $h/2$; (B) At top wall

of 12.9 dBic. The measured total efficiency and aperture efficiency are as high as up to 94% and 80%, respectively, which are a litter lower than the simulated ones of 98% and 84%. The discrepancy is due to the conductor loss of the metal material, the power loss on the sub-miniature-A port, and the machining accuracy of the antenna. The radiation patterns depicted in Figure 12 indicates that the measured co-polarization (LHCP) is almost the same with the simulated one, and the measured cross-polarization (RHCP) is better than −25 dB (The RHCP gain is about −12.4 dBic). The good agreement between the measured and simulated validates the design concept.

To show the effect of the number of slots, three antennas with 2 × 2, 3 × 3, and 4 × 4 slots in a same aperture size of $1.33\lambda_0 \times 1.33\lambda_0$ at 3.18 GHz are designed and compared, the top views are shown in Figure 13. All the three CP antennas are designed based on the same cavity modes. The comparison of the simulated results of the three antennas is provided in Table 1. It can be seen that the 4 × 4 array only has 0.1 dB higher directivity than the 3 × 3 array, but has a more complicated antenna structure. While the 2 × 2 has 0.6 dB lower directivity than the 3 × 3 array. Besides, all the three antennas have

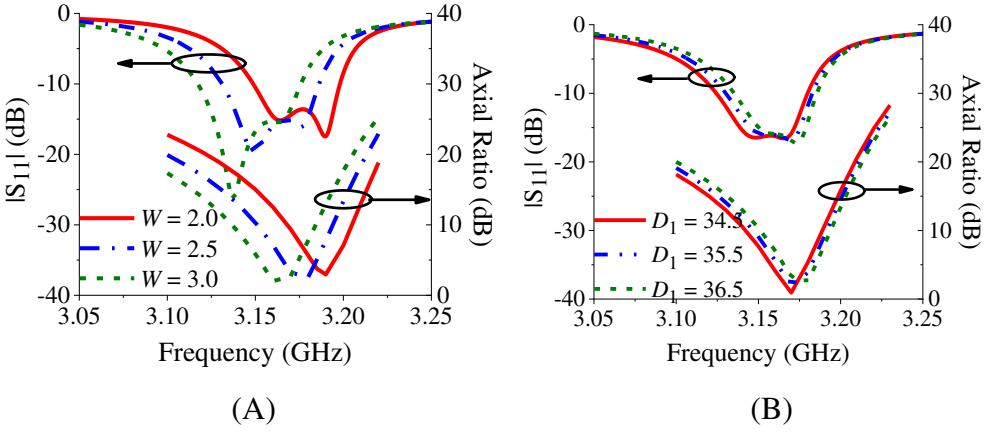

FIGURE 8 Dimensions effect on AR and $|S_{11}|$: (A) Slot width W; (B) Spacing D_1

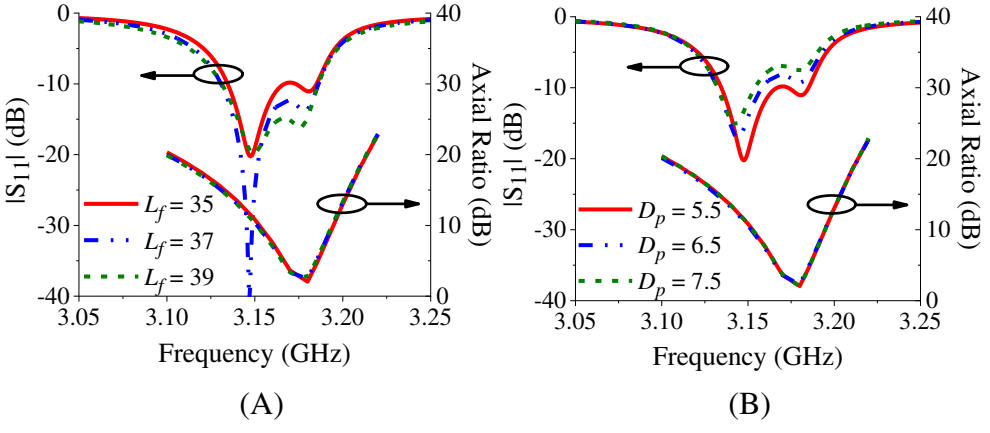

FIGURE 9 Dimensions effect on AR and $|S_{11}|$: (A) Length of feeding slot, L_f; (B) Spacing between probe and bottom wall, D_p

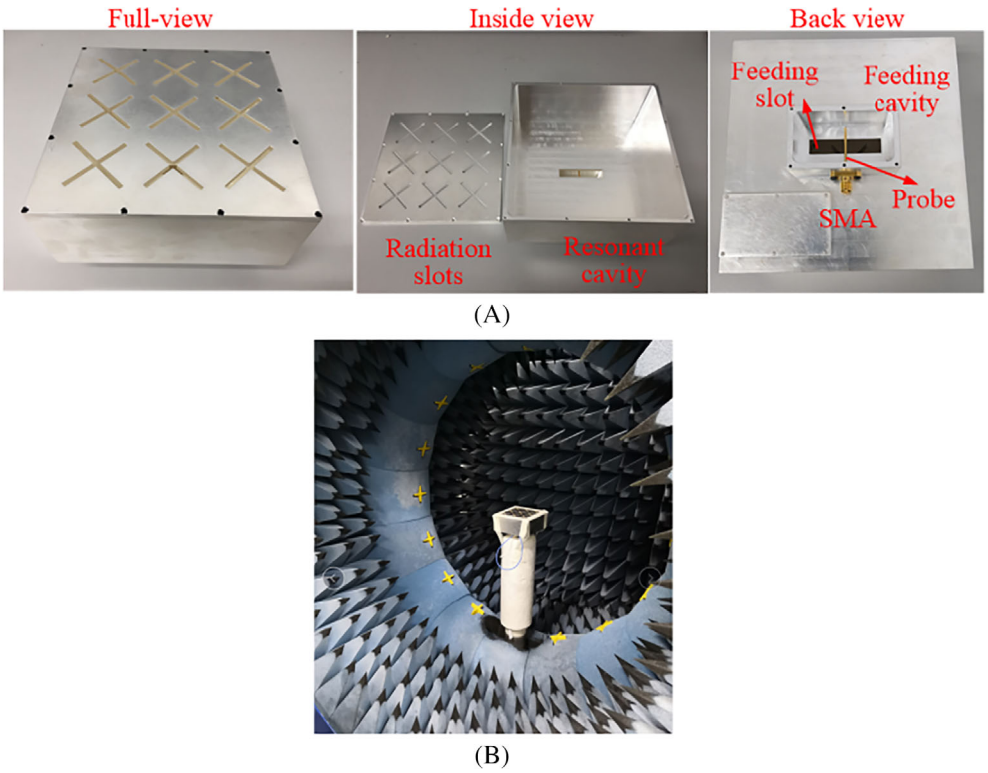

FIGURE 10 Photograph of (A) Proposed fabricated antenna and (B) Antenna under test. Final dimensions (Unit: mm): $a = 120$, $h = 49$, $L_1 = 37.5$, $L_2 = 35$, $W = 2.5$, $D_1 = 36.5$, $t_1 = 2.5$, $t_2 = 3$, $D_p = 5.5$, $W_f = 8$, $L_f = 37$, $L_p = 21.2$, $P = 48$, $q = 25$, $s = 25$

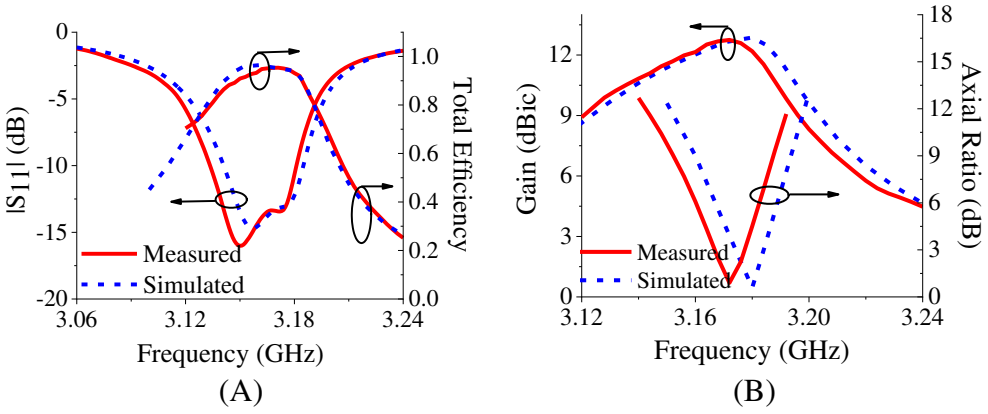

FIGURE 11 Measured and simulated results: (A) $|S_{11}|$ and efficiency; (B) Gain and axial ratio

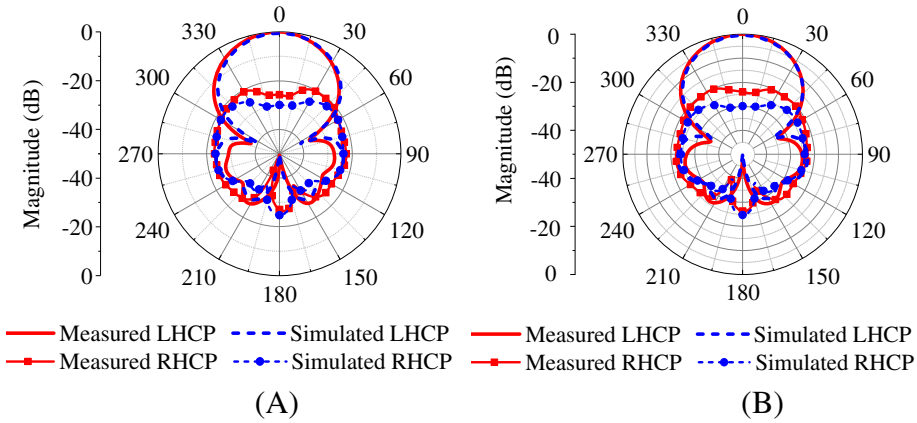

FIGURE 12 Measured (At 3.172 GHz) and simulated (At 3.18 GHz) radiation pattern: (A) $\varphi = 0°$; (B) $\varphi = 90°$

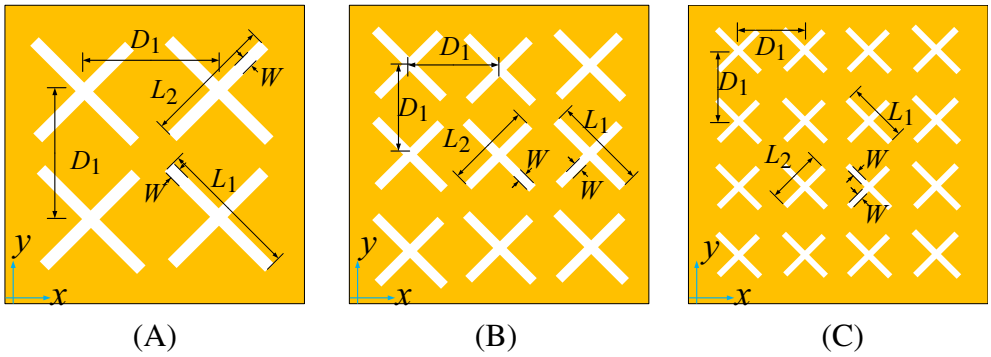

FIGURE 13 Three types of slot arrays: (A) 2 × 2 array; (B) 3 × 3 array; (C) 4 × 4 array

TABLE 1 Comparison of three types of slot antenna arrays in a same-size cavity

Array	Frequency (GHz)	Aperture size ($\lambda_0 \times \lambda_0$)	L_1 / L_2 (λ_0)	$D_1(\lambda_0)$	IBW (%)	ARBW (%)	OBW (%)	Directivity (dBic)	TE (%)	AE (%)
2 × 2	3.18	1.33 × 1.33	0.45/0.43	0.6	1.9	0.5	0.5	12.4	95	72
3 × 3	3.18	1.33 × 1.33	0.4/0.38	0.39	1.6	0.5	0.5	13	97	82
4 × 4	3.18	1.33 × 1.33	0.33/0.31	0.3	1.2	0.4	0.4	13.1	98	84

Abbreviations: AE, aperture efficiency; ARBW, AR bandwidth; IBW, impedance bandwidth; OBW, overlap bandwidth of IBW and ARBW; TE, total efficiency.

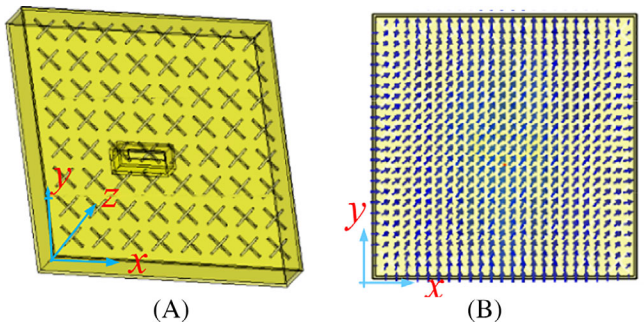

FIGURE 14 Proposed 8 × 8 CP cavity-backed slot antenna array: (A) Full-view; (B) Electric field distribution at XY-plane. Final dimensions (Unit: mm): $a = 332$, $h = 46$, $L_1 = 37$, $L_2 = 35.2$, $W = 2.5$, $D_1 = 40$, $t_1 = 2.5$, $t_2 = 3$, $D_p = 8.5$, $W_f = 12$, $L_f = 50$, $L_p = 22$, $P = 70$, $q = 27$, $s = 25$

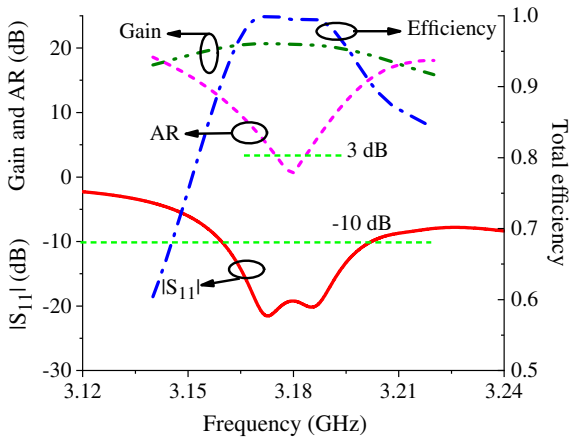

FIGURE 15 Simulated results: Reflection coefficient, AR, gain, and efficiency

similar operating bandwidth. Thus, the 3 × 3 array in such aperture size shows a good trade-off between the antenna complexity and the antenna performance. In the 3 × 3 array, the lengths of the crossed slots (L_1 and L_2) and distance (D_1) between slots are all about $0.4\lambda_0$.

4 | FURTHER DESIGN

To further show the feasibility of proposed design concept, a large-scale CP slot array with 8 × 8 cross-slots is designed. The physical structure is shown in Figure 14A, it only includes an air-filled resonant cavity, the radiation slots on the top wall and a coaxial-to-waveguide transition. The same degenerate modes are used to design CP antenna, which can be seen in Figure 14B. Similarly, all the elements of the CP array are directly fed by the electric field of the cavity modes without using any other feeding structure. The antenna's aperture size is 332 mm × 332 mm (about $3.52\lambda_0 \times 3.52\lambda_0$). The simulated results are depicted in Figure 15. It can be seen that the antenna operates at 3.18 GHz, the in-band return loss is better than 19 dB, the radiation gain is about 20.6 dBic. Besides, this antenna can achieve 99.5% total efficiency for such large antenna array, which is mainly due to the simplified feeding structure without using the power dividing network. The simulated gain and total efficiency

TABLE 2 Performance of two proposed antenna arrays

Works	State	Frequency (GHz)	$\lvert S_{11}\rvert$ (VSWR)	Gain (dBic)	AR (dB)	ARBW (%)
3 × 3	Measured	3.172	<−12 dB (1.68)	12.6	0.8	0.5
	Simulated	3.18	<−12 dB (1.68)	12.9	0.5	0.5
8 × 8	Simulated	3.18	<−19 dB (1.25)	20.6	0.6	0.35

Abbreviation: ARBW: AR bandwidth;

TABLE 3 Comparison with reported CP cavity-backed slot antennas

Reference	Frequency (GHz)	Elements	IBW (%)	ARBW (%)	OBW (%)	Cavity type	DM	PD	PS or P	Peak gain (dBic)	TE (%)	AE (%)	Size ($\lambda_0 \times \lambda_0 \times \lambda_0$)
15	10.1	1	3	0.8	0.8	SIW	Yes	N.A.	N.A.	6	N.G.	N.G.	N.G.
18	35.43	4 × 4	0.7	0.9	0.7	SIW	Yes	Yes	Yes	18.14	N.G.	47	3.3 × 3.3 × 1.8
19	5.73	1	1.63	0.44	0.44	SIW	Yes	N.A.	N.A.	6.96	N.G.	57	0.69 × 0.64 × 0.02
20	3.59	2 × 2	∼5	∼0.7	∼0.7	Full metal	Yes	No	No	8.8	N.G.	N.G.	N.G.
21	19.88	16 × 16	15.9	13.8	13.8	SIW	No	Yes	Yes	25.9	N.G.	21	11.9 × 12.6 × 0.15
24	30	16 × 16	N.G.	N.G.	16	Full metal	No	Yes	Yes	32.8	N.G.	>60	13.1 × 13.1 × 5
26	31	8 × 8	22	21.8	21.8	Full metal	No	Yes	Yes	23.5	85	41	6.6 × 6.6 × 1.7
This work	3.172	3 × 3	1.6	0.5	0.5	Full metal	Yes	No	No	12.6	94	80	1.33 × 1.33 × 0.52
This work[a]	3.18	8 × 8	1.35	0.35	0.35	Full metal	Yes	No	No	20.6	99.5	72	3.52 × 3.52 × 0.48

Abbreviations: AE, aperture efficiency; ARBW, AR bandwidth; DM, degenerate mode; IBW, impedance bandwidth; N.A., not applicable; N.G., not given; OBW, overlap bandwidth of IBW and ARBW; P, polarizer; PD, power divider; PS, phase shifter; TE, total efficiency.
[a]Simulated results.

include the conductor loss of the lossy copper. The detailed performances of the proposed 3 × 3 and 8 × 8 CP arrays are listed in Table 2.

The comparison with other reported cavity-backed slot antennas is provided in Table 3. The proposed slot antenna array (up to 8 × 8 elements) owns a simple antenna structure without using any power dividers and phase shifters/polarizers. These merits are obtained along with a narrow bandwidth, which is due to that: (1) The degenerate cavity modes[11-20] are used to achieve CP radiation (Main factor); (2) The high unloaded *Q*-factor of the rectangular cavity modes; (3) The proposed simplified feeding structure based on the electric field of the cavity modes.

5 | CONCLUSION

In this work, a novel simplified feeding structure is proposed to design the CP slot antenna arrays. The rotated cross-slots with different length serve as the CP elements, and they are directly fed by the electric field of the cavity modes without using the complicated power dividing network and phase shifters. High efficiency and simple structure of the antenna arrays are achieved by using proposed feeding technique. A measured prototype of the 3 × 3 CP slot array is presented to validate the design concept. An 8 × 8 CP slot array is also presented to show the feasibility in designing large-scale slot array, which can also achieve a high efficiency of 99.5%. Besides, due to the simple structure and individual tuning of impedance matching, the proposed design concept is easily duplicated for practical applications.

ACKNOWLEDGMENTS

This work is supported in part by the National Natural Science Foundation of China under grants 62071306 and 61801299, in part by the Natural Science Foundation of Guangdong Province under grant 2018A030313481, in part by the Shenzhen Science and Technology Program under grants JCYJ20180305124543176, JCYJ20190728151457763, GJHZ20180418190529516, and JSGG20180507183215520, in part by Shenzhen University Research Startup Project of New Staff under grant 860-000002110311.

DATA AVAILABILITY STATEMENT

All the data in this manuscript is available.

ORCID

Rui-Sen Chen https://orcid.org/0000-0001-7308-0468
Sai-Wai Wong https://orcid.org/0000-0001-5363-1576

Yin Li https://orcid.org/0000-0003-3246-4793
Yejun He https://orcid.org/0000-0002-8564-5355

REFERENCES

1. Mukherjee S, Biswas A. Compact high gain half-mode substrate integrated waveguide cavity antenna using hybrid mode. *Int J RF Microw Comput Aided Eng*. 2019;29:e21919.
2. Kumar A, Chaturvedi D, Raghavan S. Low-profile substrate integrated waveguide cavity-backed self-triplexed slot antenna. *Int J RF Microw Comput Aided Eng*. 2019;29:e21606.
3. Nigam P, Agarwal R, Muduli A, Sharma S, Pal A. Substrate integrated waveguide based cavity-backed self-triplexing slot antenna for X-Ku band application. *Int J RF Microw Comput Aided Eng*. 2020;30:e22172.
4. Parment F, Ghiotto A, Vuong T, Duchamp J, Wu K. Air-filled substrate integrated waveguide for low-loss and high power-handling millimeter-wave substrate integrated circuits. *IEEE Trans Microw Theory Tech*. 2015;63(4):1228-1238.
5. Belenguer A, Esteban H, Borja AL, Boria VE. Empty SIW technologies: a major step toward realizing low-cost and low-loss microwave circuits. *IEEE Microw Mag*. 2019;20(3):24-45.
6. Van den Brande Q, Lemey S, Vanfleteren J, Rogier H. Highly efficient impulse-radio ultra-wideband cavity-backed slot antenna in stacked air-filled substrate integrated waveguide technology. *IEEE Trans Antennas Propag*. 2018;66(5):2199-2209.
7. Yun S, Kim D-Y, Nam S. Bandwidth and efficiency enhancement of eavity-backed slot antenna using a substrate removal. *IEEE Antennas Wireless Propag Lett*. 2012;12:1458-1461.
8. Yu X, Ni D, Liu S, Li Z, Wang W. Design of a wideband waveguide slot array antenna and its decoupling method for synthetic aperture radar. Paper presented at: Proc. Eur Microwave Conf, 2008: 135–138.
9. Wu Y-M, Wong S-W, Wong H, Chen F-C. A design of bandwidth-enhanced cavity-backed slot filtenna using resonance windows. *IEEE Trans Antennas Propag*. 2019;67(3):1926-1930.
10. Yuan W, Liang X, Zhang L, Geng J, Zhu W, Jin R. Rectangular grating waveguide slot array antenna for SATCOM applications. *IEEE Trans Antennas Propag*. 2019;67(6):3869-3880.
11. Lu J, Zhang HC, Wei C, Hong J-S, Cui TJ. Design of compact circularly polarized antenna using sunshine-shaped slotted patch. *IEEE Trans Antennas Propag*. 2020;68(9):6800-6805.
12. Barad D, Mohapatra S, Behera SB, Behera S. Integrated circularly polarized microstrip antenna with dual-mode-polarization insensitive characteristics. *Int J RF Microw Comput Aided Eng*. 2020;30:e22039.
13. Re PDH, Comite D, Podilchak SK. Single-layer series-fed planar array with controlled aperture distribution for circularly polarized radiation. *IEEE Trans Antennas Propag*. 2020;68(6):4973-4978.
14. Li K, Wang F-W, Ren Y-H, Cai Y-M. Dual-band circularly polarized antenna with harmonic suppression performance. *Int J RF Microw Comput Aided Eng*. 2019;29:e21798.
15. Luo GQ, Hu ZF, Liang Y, Yu LY, Sun LL. Development of low profile cavity-backed crossed slot antennas for planar integration. *IEEE Trans Antennas Propag*. 2009;57(10):2972-2979.
16. Wu Q, Yin J, Yu C, Wang H, Hong W. Low profile millimeter-wave SIW cavity-backed dual-band circularly-polarized antenna. *IEEE Trans Antennas Propag*. 2017;65(5):7310-7315.
17. Priya S, Kumar K, Dwari S. Substrate integrated waveguide dual-frequency dual-sense circularly polarized cavity-backed slot antenna. *Int J RF Microw Comput Aided Eng*. 2019;29:e21987.
18. Li W, Tang X, Yang Y. A Ka-band circularly polarized substrate integrated waveguide cavity-backed antenna array. *IEEE Antennas Wireless Propag Lett*. 2019;18(9):1882-1886.
19. Xu Y, Wang Z, Dong Y. Circularly polarized slot antennas with dual-mode elliptic cavity. *IEEE Antennas Wireless Propag Lett*. 2020;19(4):715-719.
20. Wu Y-M, Wong S-W, Lin J-Y, Zhu L, He Y, Chen F-C. A circularly-polarized cavity-backed slot antenna with enhanced radiation gain. *IEEE Antennas Wireless Propag Lett*. 2018;17(6):1010-1014.
21. Guan DF, Ding C, Qian ZP, Zhang YS, Guo YJ, Gong K. Broadband high-gain SIW cavity-backed circular-polarized array antenna. *IEEE Trans Antennas Propag*. 2016;64(4):1493-1497.
22. Wu X, Yang F, Xu F, Zhou J. Circularly-polarized waveguide antenna with dual pairs of radiation slots at Ka-band. *IEEE Antennas Wireless Propag Lett*. 2017;16:2947-2950.
23. Gatti RV, Rossi R. A dual-polarization slotted waveguide array antenna with polarization-tracking capability and reduced sidelobe level. *IEEE Trans Antennas Propag*. 2016;64(4):1567-1572.
24. Wu J, Cheng YJ, Wang HB, Zhong YC, Ma D, Fan Y. A wideband dual circularly polarized full-corporate waveguide array antenna fed by triple-resonant cavities. *IEEE Trans Antennas Propag*. 2017;65(4):2135-2139.
25. Zhou S-G, Huang G-L, Chio T-H. A lightweight, wideband, dual-circular-polarized waveguide cavity array designed with direct metal laser sintering considerations. *IEEE Trans Antennas Propag*. 2017;66(2):675-682.
26. Akbari M, Farahbakhsh A, Sebak A-R. Ridge gap waveguide multilevel sequential feeding network for high-gain circularly polarized array antenna. *IEEE Trans Antennas Propag*. 2019;67(1):251-258.
27. Haneishi M, Yoshida S. A design method of circularly polarized rectangular microstrip antenna by one-point feed. *Electron Commun Jpn*. 1981;64-B(4):46-54.

AUTHOR BIOGRAPHIES

Rui-Sen Chen (S'13) was born in Fujian, China. He received the BS degree from Hunan University of Science and Technology, Hunan, in 2012, received the Master degree in electromagnetic field and radio technology from South China University of Technology, Guangzhou, in 2015, and received the Doctor's degree in information and communication engineering from Shenzhen University, Shenzhen, in 2021. He was a research assistant with Faculty of Science and Technology, University of Macau from January 2020 to December 2020. He is currently an

Assistant Professor with Foshan University. His current research interests include microwave filter, antenna and cavity components.

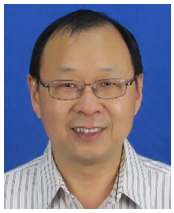

Lei Zhu (S'91-M'93-SM'00-F'12) received the BE and ME degrees in radio engineering from the Nanjing Institute of Technology (now Southeast University), Nanjing, China, in 1985 and 1988, respectively, and the PhD degree in electronic engineering from the University of Electro-Communications, Tokyo, Japan, in 1993. From 1993 to 1996, he was a Research Engineer with Matsushita-Kotobuki Electronics Industries Ltd., Tokyo, Japan. From 1996 to 2000, he was a Research Fellow with the École Polytechnique de Montréal, Montréal, QC, Canada. From 2000 to 2013, he was an Associate Professor with the School of Electrical and Electronic Engineering, Nanyang Technological University, Singapore. He joined the Faculty of Science and Technology, University of Macau, Macau, China, as a Full Professor in August 2013, and has been a Distinguished Professor since December 2016. From August 2014 to August 2017, he served as the Head of Department of Electrical and Computer Engineering, University of Macau. So far, he has authored or coauthored more than 630 papers in international journals and conference proceedings. His papers have been cited more than 10 950 times with the H-index of 54 (source: Scopus). His research interests include microwave circuits, antennas, periodic structures, and computational electromagnetics. Dr. Zhu was the Associate Editors for the IEEE Transactions on Microwave Theory and Techniques (2010–2013) and IEEE Microwave and Wireless Components Letters (2006–2012). He served as a General Chair of the 2008 IEEE MTT-S International Microwave Workshop Series on the Art of Miniaturizing RF and Microwave Passive Components, Chengdu, China, and a Technical Program Committee Co-Chair of the 2009 Asia-Pacific Microwave Conference, Singapore. He served as the member of IEEE MTT-S Fellow Evaluation Committee (2013–2015), and as the member of IEEE AP-S Fellows Committee (2015–2017). He was the recipient of the 1997 Asia-Pacific Microwave Prize Award, the 1996 Silver Award of Excellent Invention from Matsushita-Kotobuki Electronics Industries Ltd., the 1993 Achievement Award in Science and Technology (first prize) from the National Education Committee of China, the 2020 FST Research Excellence Award from the University of Macau, and the 2020 Macao Natural Science Award (second prize) from the Science and Technology Development Fund (FDCT), Macau.

Sai-Wai Wong (S'06-M'09-SM'14) received his BS degree in electronic engineering from the Hong Kong University of Science and Technology, Hong Kong, in 2003, and the MSc and PhD degrees in communication engineering from Nanyang Technological University, Singapore, in 2006 and 2009, respectively. From July 2003 to July 2005, he was an Electronic Engineer to lead an electronic engineering department in China with two Hong Kong manufacturing companies. From May 2009 to Oct. 2010, he was a Research Fellow with the ASTAR Institute for Infocomm Research, Singapore. Since 2010, he was an Associate Professor and later become a Full Professor, in the School of Electronic and Information Engineering, South China University of Technology, Guangzhou, China. From July 2016 to September 2016, he is a Visiting Professor in City University of Hong Kong. Since 2017, he has been a Full Professor with the College of Electronics and Information Engineering, Shenzhen University, Shenzhen, China. His current research interests include RF/microwave circuit and antenna design. So far, he has authored and co-authored more than 200 papers in international journals and conference proceedings. He was the recipient of the New Century Excellent Talents in University awarded by the Ministry of Education of China in 2013 and the Shenzhen Overseas High-Caliber Personnel Level C ("Peacock Plan Award" C) in 2018.

Xu-Zhou Yu received the BE degree from the school of Electronic and Information Engineering, Tianjin University (TJU), Tianjin, China, in 2019. He is currently working towards his Master's degree with the College of Electronics and Information Engineering, Shenzhen University (SZU), Shenzhen, China. His current research interests include microwave cavity circuit design.

Jing-Yu Lin (S'14) received the BE degree from Southwest Jiaotong University (SWJTU), Chengdu, China, in 2016, and the ME degree at the school of Electronic and Information Engineering, South China University of Technology (SCUT), Guangzhou, China, in 2018. He is currently working towards PhD

degree in University of Technology Sydney (UTS), Ultimo, Australia. From October 2017 to February 2019, he was as an exchange student in University of Technology Sydney, Ultimo, Australia. His current research interests include microwave cavity circuit design.

Yin Li (M'19) received the BS degree in applied physics from China University of Petroleum, Dongying, China in 2009, M. Eng. in electromagnetic field and microwave technology from University of Electronic Science and Technology of China (UESTC), Chengdu, China, in 2012, and the PhD degree in with the University of Macau, Macau, China. P. He is currently a post doctor fellow with school of electronics and information from Shen Zhen University, Shen Zhen, China. From 2013 to 2015, he was a Research Assistant with University of Hong Kong (HKU), Hong Kong, China. His current research interests include numerical modeling methods of passive microwave circuits, computational electromagnetics, and microwave circuits, frequency selectivity surface, filtering antenna.

Yejun He (SM'09) received the PhD degree in information and communication engineering from Huazhong University of Science and Technology (HUST), Wuhan, China, in 2005. From 2005 to 2006, he was a Research Associate with the Department of Electronic and Information Engineering, Hong Kong Polytechnic University, Hong Kong. From 2006 to 2007, he was a Research Associate with the Department of Electronic Engineering, Faculty of Engineering, Chinese University of Hong Kong, Hong Kong. In 2012, he was a Visiting Professor with the Department of Electrical and Computer Engineering, University of Waterloo, Waterloo, ON, Canada. From 2013 to 2015, he was an Advanced Visiting Scholar (Visiting Professor) with the School of Electrical and Computer Engineering, Georgia Institute of Technology, Atlanta, GA, USA. Since 2011, he has been a Full Professor with the College of Electronics and Information Engineering, Shenzhen University, Shenzhen, China, where He is the Director of Guangdong Engineering Research Center of Base Station Antennas and Propagation, and the Director of Shenzhen Key Laboratory of Antennas and Propagation, Shenzhen, China. He was awarded as Pengcheng Scholar Distinguished Professor, Shenzhen, China. He was also a recipient of the Shenzhen Overseas High-Caliber Personnel Level B ("Peacock Plan Award" B) and Shenzhen High-Level Professional Talalent (Local Leading Talent). He received the Shenzhen Science and Technology Progress Award and the Guangdong Provincial Science and Technology Progress Award. He has authored or coauthored more than 200 research papers, books (chapters) and holds about 20 patents. His research interests include wireless communications, antennas and radio frequency. Dr. He is serving as Associate Editor of IEEE Network, International Journal of Communication Systems, China Communications, as well as Wireless Communications and Mobile Computing. He served as General Chair of IEEE ComComAp 2019. He has served as a Reviewer for various journals such as IEEE Transactions on Vehicular Technology, IEEE Transactions on Communications, IEEE Transactions on Wireless Communications, IEEE Transactions on Industrial Electronics, IEEE Transactions on Antennas and Propagation, IEEE Antennas and Wireless Propagation Letters, IEEE Wireless Communications, IEEE Communications Letters, IEEE Journal on Selected Areas in Communications, International Journal of Communication Systems, Wireless Communications and Mobile Computing, and Wireless Personal Communications. He has also served as a Technical Program Committee Member or a Session Chair for various conferences, including IEEE Global Telecommunications Conference (GLOBECOM), IEEE International Conference on Communications (ICC), IEEE Wireless Communication Networking Conference (WCNC), IEEE Vehicular Technology Conference (VTC), IEEE International Symposium on Antennas and Propagation (APS), European Conference on Antennas and Propagation (EuCAP), and Asia-Pacific Microwave Conference (APMC). He is the Principal Investigator for over 30 current or finished research projects including NSFC of China, the Science and Technology Program of Guangdong Province as well as the Science and Technology Program of Shenzhen City. He is a Fellow of IET, and the Chair of IEEE Antennas and Propagation Society-Shenzhen Chapter.

How to cite this article: Chen R-S, Zhu L, Wong S-W, et al. Circularly-polarized cavity-backed slot antenna array with simplified feeding structure. *Int J RF Microw Comput Aided Eng*. 2021;31(10): e22859. https://doi.org/10.1002/mmce.22859